Environmental Research xxx (xxxx) 112579

Contents lists available at ScienceDirect

Environmental Research

journal homepage: www.elsevier.com/locate/envres

Could soluble minerals be hazardous to human health? Evidence from fibrous epsomite

Matteo Giordani [a, *], Maria Assunta Meli [b], Carla Roselli [b], Michele Betti [b], Fabio Peruzzi [c], Marco Taussi [a], Laura Valentini [b], Ivan Fagiolino [d], Michele Mattioli [a]

[a] Department of Pure and Applied Sciences, University of Urbino Carlo Bo, Urbino, Italy
[b] Department of Biomolecular Sciences, University of Urbino Carlo Bo, Urbino, Italy
[c] Speleological Federation of the Emilia-Romagna Region, Bologna, Italy
[d] Gruppo C.S.A. spa, Via al Torrente 22, Rimini, Italy

ARTICLE INFO

Keywords:
Toxicity
Magnesium sulphate
Polonium
Fibres inhalation
Toxic elements

ABSTRACT

From a toxicological point of view, particulates and fibres with high solubility in water and/or in biological environments have not been considered in detail and the knowledge to date in this area is very scarce. In this study, the water-soluble natural epsomite fibres from Perticara Mine (Italy) were investigated using SEM-EDS, XRPD, ICP-AES and alpha spectrometry measurements which were combined and integrated to characterise the fibres' morphology, crystal chemistry and mineralogy. The morphological and morphometric results showed that most of the fibres are of inhalable size (D_{ae} 5.09 μm) and can be potentially adsorbed from all parts of the respiratory tract. Chemical analysis reveals significant amounts of toxic elements (As, Co, Fe, Mn, Ni, Sr, Ti, Zn) and surprisingly high contents of radioactive isotopes (^{210}Po and ^{228}Th) in epsomite crystals, making the inhalation of these fibres potentially hazardous to human health. Through this study, we want to focus on soluble minerals, such as epsomite, which can be present in both natural and anthropic environments and have never been considered from the point of view of their potential hazard.

1. Introduction

In recent years, scientists' interest in particulate matter (PM) and fibrous minerals has significantly increased, mainly because they could be potentially dangerous to human health. PM has been demonstrated to be hazardous to human health and the critical factors are primarily related to its size and chemical composition (Schwartz et al., 1996; EPA, 1996). Fibrous minerals have assumed great importance over the last few decades, especially those that can be able to release very small fibres and fibrils in the range of inhalable size; they are mostly considered for regulatory purposes (length >5 μm, diameter <3 μm, diameter-length ratio >1:3; World Health Organization, 1986), because they could be potentially dangerous to human health. In particular, the most studied mineral fibres are the six asbestos minerals chrysotile, amosite, crocidolite, tremolite asbestos, actinolite asbestos and anthophyllite asbestos (e.g., World Health Organization, 1986; Boulanger et al., 2014; Andujar et al., 2016; Gualtieri, 2017). Moreover, there are other noteworthy mineral fibres, such as fibrous antigorite and balangeroite (Groppo et al., 2005; Cardile et al., 2007; Petriglieri et al., 2021); the amphiboles winchite, richterite and fluoro-edenite (National Institute for Occupational Safety and Health, 2011; Gianfagna et al., 2003); the zeolites erionite, offretite, ferrierite, mesolite, thomsonite and mordenite (e.g., Giordani et al., 2016, 2017, 2021; Cangiotti et al., 2017; Gualtieri et al., 2018a; Mattioli et al., 2018; Di Giuseppe, 2020); and also talc and clay minerals (e.g., sepiolite and palygorskite; García-Romero and Suárez, 2013; Larson et al., 2016).

The first factor to consider in assessing the risk of exposure to PM and fibrous minerals is their respirability, i.e., the capacity of these particles to be inhaled through the nose and/or mouth and enter into the lungs. The penetration capacity of a particle into the lungs depends primarily upon a size parameter called the equivalent aerodynamic diameter (D_{ae}), i.e., the diameter of a sphere with a unit density of 1.0 g/cm^3 with aerodynamic characteristics identical to those of the particle of interest (World Health Organization, 1999; Sturm and Hofmann, 2009). The aerodynamic diameter of airborne PM can range from a few nanometres up to 100 μm. Furthermore, the inhalable particles smaller

* Corresponding author. University of Urbino Carlo Bo, Department of Pure and Applied Sciences, Scientific Campus E. Mattei, Via Ca' Le Suore 2/4 61029, Urbino, Italy.
E-mail address: matteo.giordani@uniurb.it (M. Giordani).

https://doi.org/10.1016/j.envres.2021.112579
Received 8 September 2021; Received in revised form 3 December 2021; Accepted 12 December 2021
0013-9351/

than 10 μm (referred to as PM_{10}) can reach deeper parts of the lungs and are considered very dangerous (Schwartz et al., 1996). For this reason, particles with aerodynamic diameters up to 2.5 μm ($PM_{2.5}$) are the most dangerous (Miller et al., 1979; EPA, 1996). Regarding particle deposition, the human respiratory system is divided into the (i) extrathoracic region, (ii) tracheobronchial tree and (iii) alveolar or pulmonary region, with the latter being the most important for PM retention and pulmonary diseases (Salma et al., 2002; Brown et al., 2013). Additionally, fibre biopersistence, which is strictly related to the chemical composition, and other features such as the structure, net charge, microtopography, surface area, zeta potential and interacting capability constitute other very important factors related to the toxicity and carcinogenicity of the fibres (Hochella, 1993; Hesterberg et al., 1998; Fubini, 2001; Maxim et al., 2006; Pollastri et al., 2014; Ballirano et al., 2015; Bloise et al., 2016; Crovella et al., 2016; Mattioli et al., 2016a; Cangiotti et al., 2017, 2018; Pacella et al., 2018; Giordani et al., 2019, 2021).

In the realm of studies of particle and fibre health effects, a significant branch of particulate and fibrous minerals with high solubility in water and/or in biological environments has not been considered, and the knowledge to date about these minerals is very scarce. In this case, the features, processes and involved reactions are completely different from those of biopersistent particles and fibrous minerals such as asbestos and erionite. Unlike insoluble particles, for which the deposition site in the respiratory system is of paramount importance, very soluble substances can be adsorbed from all parts of the respiratory tract, so the site of deposition seems to be of less importance (World Health Organization, 1999), even if no specific studies discussing this are present in the literature. However, the deposition area could become significant in the case of insoluble fractions bounded to soluble particles, or in the case of hazardous compounds forming the soluble particles itself. In fact, it has been observed that the toxic metals and water-soluble organic fraction in $PM_{2.5}$ are easily absorbed by the human body (Ventura et al., 2017). Oberdörster (1988) suggests that 'biologically inert' particles do not exist, and that any particle at sufficiently high lung burdens can cause lung damage. For this reason, the fact that the biopersistence of some mineral fibres is low or even negligible does not exclude them from being potentially dangerous for humans in other ways.

With regard to inhalable soluble particles, a complete chemical and structural characterisation is of fundamental importance for knowing the fibre characteristics and understanding (and predicting) the type and amount of solute that originates during the *in-vivo* solubilisation processes. Furthermore, it is also important to assess the solute-related effects in the biological environment (e.g., cells and lungs), especially when fluids are in contact with sensitive (reactive) cells and tissue. A critical aspect is that the soluble particulate could also generate pulmonary toxicity (Adamson et al., 1999; Oberdörster, 1988). Within the lung, the tracheobronchial tree area is mainly cleared by adsorptive mechanisms, but mechanical clearance along the mucociliary escalator or coughing also can contribute to the clearance of inhaled solutes. Meanwhile, transepithelial transport is the major mechanism for clearance of the alveolar region (Oberdörster, 1988). Lipophilicity, hydrophilicity and the molecular size are the major determinants of the rate of the absorptive processes of the solutes, and water-soluble substances that reach the interstitium are cleared by diffusion into blood capillaries and to a lesser degree into lymph capillaries (depending on their molecular size). Binding to epithelial or interstitial cell structures and adsorption onto insoluble particles can occur and significantly increase retention from minutes or hours to days and months (Oberdörster, 1988).

This work aims to shed new light on the toxicological role that epsomite, a common fibrous soluble mineral present both in natural and anthropic environments, can play in human health. Epsomite is widespread in the Earth's crust and generally occurs as an efflorescence in botryoidal to reniform masses or crusts; it more rarely occurs as crystals with a fibrous to woolly habit (Ruiz-Agudo et al., 2008; see the Supplementary Material for the mineralogical background of epsomite). Epsomite occurs mainly on the ground and in the exposed walls of mines and caves (Ribeiro et al., 2013; Del Rio-Salas et al., 2019; Nieva et al., 2021), on outcrops of sulphide-bearing magnesian rocks (e.g., dolostones and serpentinites; Navarro et al., 2021), as a product of evaporation at mineral springs and saline lakes and rarely as fumarolic sublimate (Anthony et al., 1990; Biagioni et al., 2020). Additionally, epsomite is often present as white efflorescence on bricks, concrete, artificial stones and joint mortars in modern buildings (e.g., Maguregui et al., 2010; Morillas et al., 2015). Natural epsomite is also widely used in many fields. It is used in agriculture as fertilizer, in the manufacturing of cotton and silk, in ore processing and in the explosives industry; it is a source of magnesium in some manufacturing processes, and it has applications in the field of dosimetric measurements. Moreover, epsomite has numerous medical and pharmaceutical applications; for example, it is used in the treatment of cardiac arrhythmia, acute asthma, eclampsia and gallstones (Ruiz Agudo et al., 2008 and the references therein).

Epsomite from Perticara Mine (Central Italy) was selected because it is a highly soluble mineral in water that perfectly highlights the process we want to focus on, but also because of its very fibrous habit, its abundance and its purity. In addition, many diseases were known to occur in the workers of the Perticara Mine (e.g., lung diseases, anaemia) but due to the lack of specific studies, no cause-and-effect relationship is known at the moment. However, in the area of the village of Perticara, some cases of leukaemia and sterility in the inhabitants and descendants of miners are known (personal communication). The potential hazards associated with epsomite have not been considered previously and this study represents a first step towards understanding a limited research field.

Here, natural epsomite crystals with a fibrous habit have been studied in detail using scanning electron microscopy with energy dispersive spectroscopy (SEM-EDS), X-ray powder diffraction (XRPD), inductively coupled plasma atomic emission spectroscopy (ICP-AES) and alpha spectrometry measurements. The collected data were combined and integrated to characterise the epsomite from the morphological, crystal-chemical, mineralogical and radiological points of view. The obtained results showed that there are morphological similarities between epsomite and elongated mineral particles (EMPs) of concern and indicate that the presence of trace elements and radioactive isotopes could contribute to a carcinogenic mechanism in the pulmonary system.

2. Materials and methods

2.1. Materials

A representative sample of natural epsomite crystals (labeled MP) with a fibrous habit (general formula $Mg(SO_4)\cdot 7H_2O$) was collected in the abandoned Perticara sulphur mine in the Rimini province (Central Italy, Fig. 1).

The mine was developed in the Gessoso-Solfifera Formation, a rock succession mainly formed by gypsum and limestone that is well preserved in the western Romagna Apennines area (Roveri et al., 2003). The Gessoso-Solfifera Formation comprises primary and clastic, resedimented evaporites with interbedded organic-rich shales, which were deposited during the evaporitic and post-evaporitic stages of the Messinian salinity crisis (Roveri et al., 2003). Here, the epsomite fibrous crystals grow extensively on both the rock walls and blocks of the mine (Fig. 2). After collection, the sample was stored at room temperature (about 20 °C, comparable to the temperature of the mine) in airtight containers to prevent modifications or alteration, such as dehydration/hydration and the phase changes of the material. Pure fibres and needles of epsomite were selected by binocular microscopy and prepared for subsequent analysis.

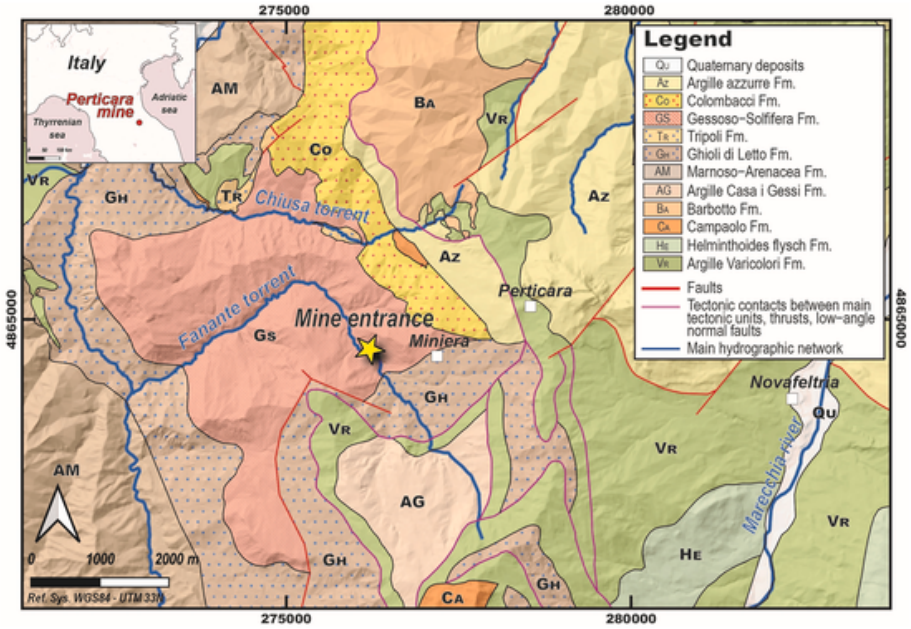

Fig. 1. Geological sketch map of the Perticara Mine. The yellow star indicates the entrance of the Perticara Mine (modified from Conti et al., 2020).

Fig. 2. Images of epsomite crystals from Perticara Mine. Abundant, centimetric size bundles and crystals growing on rocks with different orientation.

2.2. Methods

2.2.1. Scanning electron microscopy (SEM)

Morphological observations and micro-chemical characterisation were performed using an environmental scanning electron microscope FEI Quanta 200 FEG (FEI, Hillsboro, OR, USA) that was equipped with an energy-dispersive X-ray spectrometer (EDS) for qualitative and semi-quantitative microchemical analyses. The operating conditions were a 25 kV accelerating voltage, variable beam diameter, 10–12 mm working distance and 0° tilt angle. The SEM low vacuum mode was used, with the specimen chamber pressure set from 0.80 to 0.90 mbar. The images were obtained using a single-shot detector (SSD).

The dimensions of the individual fibres were measured directly on several SEM microphotographs. The widths and lengths of more than three thousand fibrils were measured. Chemical data were collected at several analytical points on different epsomite crystals to check homogeneity in composition. Additional chemical analyses were also performed on impurities detected on the crystals' surfaces to determine their major element compositions.

2.2.2. Fibre density and aerodynamic diameter

The inhalability and the deposition region of a mineral fibre in the respiratory tract is related directly to its equivalent aerodynamic diameter (D_{ae}) (Heyder et al., 1986). For the calculation of D_{ae}, the fibre's density represents a fundamental parameter. Particles with $D_{ae} < 100$ μm (inhalable fraction) are deposited in the nasopharyngeal tract, particles with $D_{ae} < 10$ μm pass the larynx (thoracic fraction) and particles with $D_{ae} < 4$ μm (respirable fraction) may reach the alveoli (European Committee for Standardization, 1993). The theoretical density of epsomite MP was obtained using the following formula: (molecular weight * number of molecules per unit cell)/(unit cell volume * Avogadro's number). For the D_{ae} calculation, the equation of Gonda (1985) was used, where d = the fibre diameter; β = the fibre length/d (aspect ratio); ρ = the density; and ρ0 = the unit density (1 g/cm^3).

2.2.3. X-ray powder diffraction (XRPD)

A representative amount of pure epsomite crystals was disaggregated and carefully pulverised in an agate mortar, and the powder was loaded in a 0.7 mm side-opened aluminum sample holder. XRPD data were collected using a Philips X'Change PW1830 powder diffractometer. The analytical conditions were a 35 kV accelerating voltage and 30 mA beam current, with CuKα radiation (λ = 1.54506 Å). Data were collected in a Bragg-Brentano geometry from 2 to 65° 2Θ, with a step size of 0.01° 2Θ and a 2.5 s counting time for each step to obtain patterns of high intensity. The diffractometer is equipped with a compensating slit with a maximum divergence angle of 1°, a receiving slit of 0.2 mm and a graphite crystal monochromator. Moreover, semi-

quantitative XRPD analyses were performed. The following software packages were used for the measurements and subsequent analysis: X'Pert Quantify for data collection and instrument control, and X'Pert HighScore Plus (PANalytical, version 3.0) for semi-quantitative phase analysis, with a PDF2 reference database implemented in the software. Quartz was used as an internal calibration standard. Variations in half-height peak widths among the patterns recorded for each sample at different times are within ±2% of the mean value. Three repeated measurements were carried out for each sample. Additional XRPD data were also collected on a representative portion of the rock matrix of the epsomite crystals under the same analytical conditions.

2.2.4. Inductively coupled plasma atomic emission spectrometry (ICP-AES)

The elemental composition of the epsomite sample was determined by inductively coupled plasma-atomic emission spectrometry (ICP-AES) and atomic absorption (AS).

The sample dissolution was carried out using the EPA 3052 1996 method: 100 mg of dry samples were digested in a mixture of 9 ml of HNO_3, 3 ml HCl and 2 ml HF concentrated for 15′ at 180 °C after the addition of 10 ml H_3BO_3 at 5% for 20' at 150 °C in a block digestor DigiPREP MS (SCP Science, Canada) and filtrate. All chemicals used in sample treatment were of suprapur grade; ultrapure water was used for all solutions. The elemental determination was carried out using two methods: EPA 7473 2007 for Hg and EPA 6010D 2018 for the other elements. The EPA 7470A 2007 method is based on the absorption of radiation at 253 nm by Hg vapor. The Hg is reduced to the elemental state and aerated from solution in a closed system. The Hg concentration was measured by atomic absorption spectrophotometer (SpectrAA220, Varian, California).

With the EPA 6010D 2018 method, after sample dissolution, the originating solutions were analysed by ICP-AES, a useful multielement technique, with broad dynamic concentration ranges, high selectivity and sensitivity and low analytical limits.

A quality control check was performed to consider the possible impurity of reagents and release from containers and instrumentation. To do this, a blank sample was prepared by mixing all reagents and applying the same procedures without adding the samples. Interferences need to be assessed and valid corrections applied, or data needs to be flagged to indicate problems.

The method's accuracy was verified using recovery tests with a Laboratory Control System (LCS) constituted by a blank sample with known quantities of analytes added to it (reference sample). A difference by 20% of the mean results from the expected values was obtained by replicate preparation and the analysis of the reference sample (analytical standard errors). The reproducibility of metal determinations (precision), based on variation in the analysis of replicates on the same sample, was 10% lower.

2.2.5. Radioanalytical method for ^{210}Po

The ^{210}Po determination was based on its spontaneous deposition on a silver disk. The sample (0.1 g dry weight) was mixed at 80 °C with HCl 1 M solution for a complete dissolution. After the addition of the known activity of ^{209}Po as the yield internal standard and ascorbic acid to eliminate the ferric ion interference, polonium was deposited at 85–90 °C and pH 1.5–2, for 4 h on a silver disk.

No preliminary separation was required, and quantitative recoveries were calculated by using a standard ^{209}Po tracer. The isotopes ^{210}Po and ^{210}Pb are not necessarily in radioactive equilibrium in samples. To determine the activity concentration of ^{210}Pb, two polonium depositions are needed (Meli et al., 2019). To enable the transition from ^{210}Pb to ^{210}Po, all solutions from deposition are stored for at least 6 months for further investigation on its source. When this time has elapsed, it is possible to indirectly determine the activity of ^{210}Pb from the activity of ^{210}Po. The measurements of the polonium (counting time = 3000 min) were carried out using an α-spectrometer equipped with a semiconductor silicon detector of the surface barrier type (an active surface of 450 mm^2, resolution of 18 keV, counting efficiency of 28.0 ± 2.8% and $2{\cdot}10^{-6}$ s^{-1} of the background in the energy region of interest; Canberra Industries, Inc., 800 Research Parkway, Meriden, CT 06450) connected to a computerised multichannel analyser. The mean chemical yield for polonium was 78.4 ± 7.7%. The accuracy of the radioanalytical method was regularly checked through a) participation in intercomparison exercises organised by the International Atomic Energy Agency (IAEA) and b) the analysis of the certified reference materials IAEA-447. The averaged analytical errors were below 15% with respect to the reported activity concentrations for the certified materials. The reproducibility of the method (precision) was evaluated by carrying out replicated analyses.

2.2.6. Radioanalytical method for uranium and thorium

Uranium and thorium were separated by extraction chromatography using diamyl amylphosphonate (DAAP) as the extractant; this is a selective extractant in a nitric medium for tetravalent and hexavalent actinides (Th, U, Pu, Np) (Thakkar, 2001). After the addition of the known activity of ^{236}U and ^{229}Th as the yield internal standards in a solution of 1M $Al(NO_3)_3$ in 5M HNO_3 containing 20 mg of epsomite, chromatographic separation was carried out by DAAP column (UTEVA Resin, Eichrom Technologies); thorium was eluted by 5M HCl and uranium by 0.02M HCl. The elution solutions were evaporated, dried and mineralised; finally, the residues were dissolved in concentrated H_2SO_4 for the electroplate deposition of uranium and thorium from an ammonium sulphate solution at a pH of 4.

The uranium and thorium isotopes' alpha emitters were measured using an alpha spectrometry system with silicon detectors (Canberra, USA). The thorium mean chemical yield was 60.0 ± 7.0%. The minimum detectable concentration was $1.0{\cdot}10^{-2}$ Bq/g for uranium and $1.0{\cdot}10^{-3}$ Bq/g for thorium.

A blank sample was also prepared for the quality control of the determination of the radioactive elements. The uncertainties of the ^{210}Po and ^{228}Th measurements were calculated by considering the calibration efficiency and the peak and background statistical fluctuations. The accuracy of the radioanalytical method was regularly checked by participating in inter-comparison exercises (organised by the International Atomic Energy Agency) and analysing the certified reference materials (IAEA-414 and IAEA-327). The mean analytical standard errors were below 10% in comparison to the reported activity concentrations for the certified material. The reproducibility of the method, evaluated by carrying out replicated analyses on the same sample, was 10% lower.

3. Results

3.1. Morphology

Epsomite crystals from the MP sample have a habit ranging from prismatic/acicular to fibrous (Fig. 2). The fibres and needles are often grouped in bundles with lengths up to 4 cm that grow mainly perpendicularly to the rock surfaces. Some bundles are closely linked, showing a compact and silky appearance of centimetric dimensions, while the long single needles generally show a rigid and fragile behaviour. However, sometimes some of these fibres are curved and seem to behave in a ductile way.

In the SEM images, both bundles of fibres and single crystals were observed (Fig. 3).

The bundles are variable in thickness, but medially they are about 50 μm thick with variable lengths from 150 μm to a few hundred μm. They are composed of several prismatic to acicular crystals that are well separated from each other, but in some cases, the distinction of prismatic cleavage is less clear. Single prismatic to acicular crystals of very variable size are also present in the sample (Fig. 3a and b). Larger individuals range from less than 0.5 μm–22 μm in terms of width, with

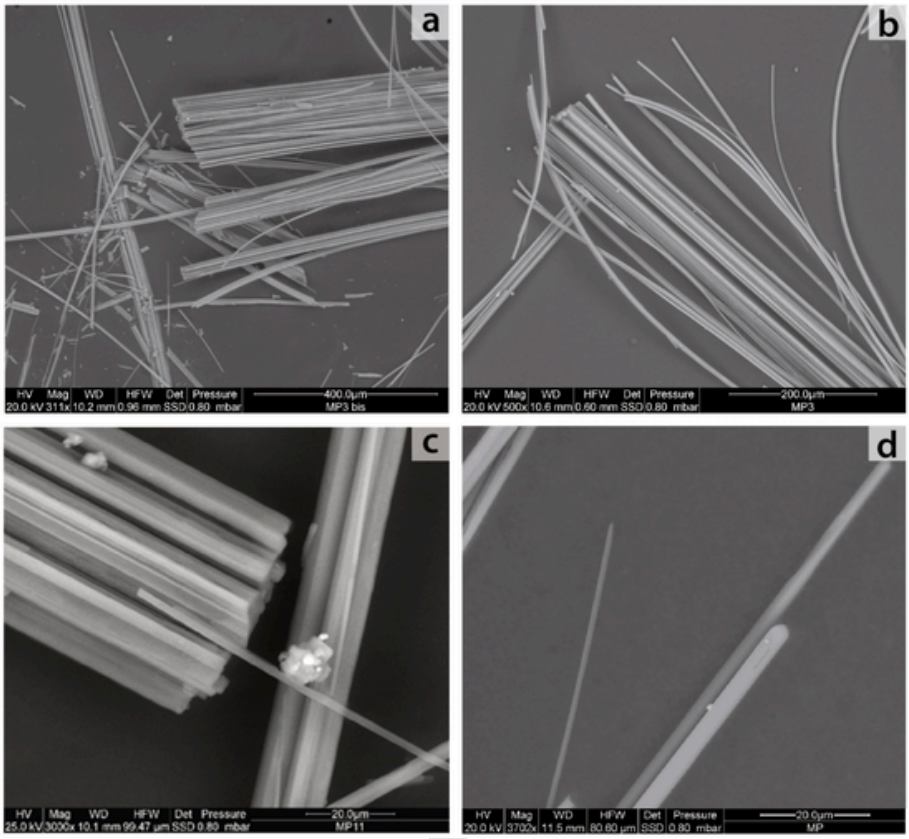

Fig. 3. Electron microphotographs of a) bundles and needles of epsomite crystals from Perticara Mine; b) particular of acicular to fibrous curved crystals; c) fibres of epsomite crystals and small particles on their surfaces; d) particular of small fibres with rounded termination.

most crystals having a width of about 4 μm (Fig. 3c and d). In terms of length, the variability is more evident: the length of the bundles varies from 30 μm to more than 800 μm, while single fibres are usually shorter (from 4.8 μm to 260 μm; 80 μm on average) and highlight a fragile physical behaviour. However, some thin needles show a curved appearance and testify to a bending ability or curved growth (Fig. 3b). Small single fibrils show no further traces of cleavage, and the resulting appearance is compact. Moreover, the terminations of the needles have rounded ends and no geometries are recognizable (Fig. 3d).

The crystals' surfaces are sometimes covered by fragments of regular geometry (epsomite remains) and irregular, very small particles and nanoparticles with different compositions as observed from the diverse electron scatter in SEM images (Fig. 3c and d).

The size of the observed fibres was measured and the results are shown in Table 1. About 25% of the measured fibres have a very small width (≤3 μm), while about 44% of fibres are within the range of 3.1–5 μm. The remaining 30% have width values bigger than 5 μm. In terms of length, almost half (48.03%) of the measured fibres are in the range from 20 μm to 100 μm. A small number of fibres are shorter than 20 μm (13.11%) while the remaining fibres are longer than 100 μm (38.85%).

Table 1
Summary of MP epsomite fibres measurements. Different range sizes of width and length of measured fibres and related percentage were reported, as well as minimum (min), maximum (max) and standard deviation (σ).

WIDTH		LENGHT	
≤3 μm	25.10%	<20 μm	13.11%
3.1–5 μm	44.40%	20–100 μm	48.03%
>5 μm	30.50%	100–200 μm	32.07%
min	0.5 μm	>200 μm	6.78%
max	22 μm	min	4.8 μm
σ	4.79	max	260 μm
		σ	63

D_{ae} has been calculated for the epsomite MP sample. By applying the equation of Gonda (1985) to epsomite fibres with a theoretical density ρ = 0.42 g/cm^3, a mean length = 80 μm and a mean diameter (d) = 4.2 μm, a D_{ae} of 5.09 μm is obtained. Accordingly, we can assume that the fraction of measured fibres that can penetrate the respiratory tract is not negligible and that the epsomite fibres of the MP sample can easily penetrate and be deposited in the laryngeal and bronchial respiratory tract.

3.2. Mineralogical composition

The resulting XRPD pattern of the analysed fibrous crystals, as shown in Fig. 4a, is consistent with a pure heptahydrate magnesium sulphate phase, i.e., epsomite. From the XRPD patterns, we can observe that the three strongest peaks are concerned with the (hkl) indices (020), (120) and (220). The highest peak intensity occurs at 2Θ ~21°, which corresponds to a d-spacing value of 4.21 Å and refers to the (220) plane. At the same time, the two secondary reflections (0.25) are positioned at 2.67 Å and 5.34 Å, respectively. Other significant peaks are positioned at values of d-spacing of 5.99 Å, 2.08 and Å, 2.75 Å. Further smaller reflections of the epsomite phase were detected at the d-spacing positions of 2.97 Å, 3.79 Å, 4.40 Å, 2.21 Å and 3.45 Å.

The XRPD pattern obtained from the rock matrix where epsomite crystals grow shows the presence of different minerals (Fig. 4b). The most represented crystalline phase is gypsum, and minor quartz, dolomite and illite-mica, which is probably represented by muscovite, are also present.

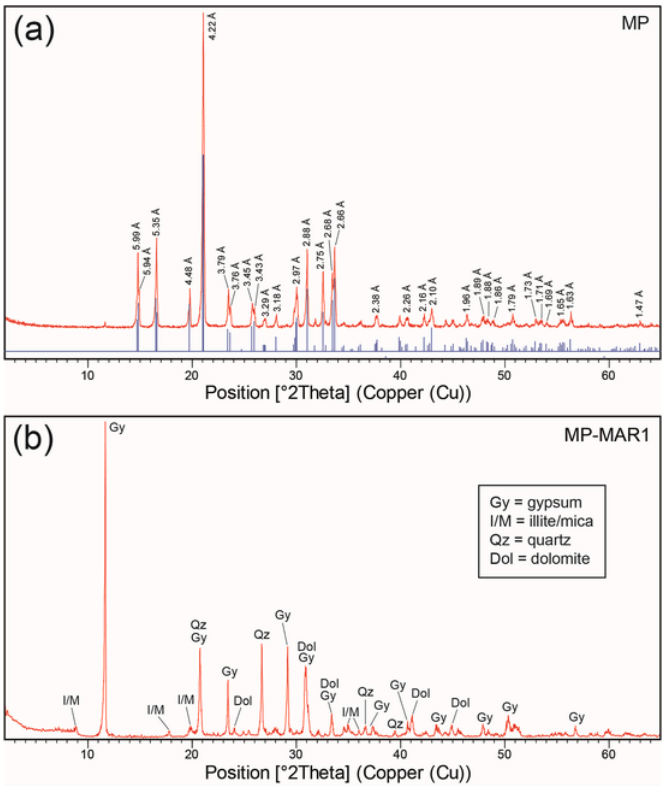

Fig. 4. XRPD spectra of a) MP sample: almost pure epsomite crystals (only very small amount of gypsum are also recognizable); b) rock matrix (MP-MAR1) sample: gypsum with minor amounts of quartz, dolomite and illite-mica were recognized.

3.3. SEM-EDS chemical composition

Data collected by EDS on pure fibrous crystals of epsomite from the MP sample show a homogeneous composition (Table 2) of sulphur trioxides in the range from 32.45 to 33.45 wt% (average value = 32.93 wt%) and magnesium oxides ranging from 16.28 to 16.44 wt% (average value = 16.34 wt%). The water content, calculated by difference, is in the range from 50.11 to 50.95 wt%, with an average value of 50.73 wt%. The data collected on epsomite crystals show low composition variability, and they are very similar to those reported by Anthony et al. (1990).

It is important to note that very small particles of impurities have been observed on the surfaces of some epsomite crystals. They show a heterogeneous composition: most of them are composed of calcium sulphate (gypsum), Fe-sulphur (pyrite), native sulphur (S) and traces of Mn and Fe (probably related to the oxide mineral group).

3.4. ICP-AES chemical composition

To define the complete chemical composition of the investigated raw epsomite sample, ICP-AES analyses were performed. This is relevant to evaluating the type and concentrations of chemical elements that can be potentially vehicolated in the lungs.

Table 2
Chemical composition of MP epsomite fibres (average value and standard deviation) from SEM-EDS analysis. H_2O content calculated by difference.

MP	Average	St. Dev.
MgO	16.34	0.07
SO_3	32.93	0.38
H_2O	50.73	0.43

Table 3
Major and minor elements concentrations of MP epsomite fibres by ICP-AES analysis. The limits of detection (LODs) (mg/kg w.w.) are presented.

Sample	MP-epsomite (mg/Kg)		
Al	100	Cu	<1
Sb	<5	Si	204
As	3,00	Sn	<0,2
Ba	<0,5	Sr	7,2
Cd	<0,5	Tl	<0,1
Ca	1030	Te	<0,5
Co	0,500	Ti	5,30
Cr (tot)	<1	Th	<5
Fe	94	Zn	18,4
P	7,2	S	127,000
Mg	77,000	Ce	<10
Mn	36,0	La	<1
Ni	11,0	Rb	<1
Pb	<0,5	U	<1
K	120	Hg	<0,0005

The ICP-AES results (Table 3) showed sulphur and magnesium as major chemical constituents (127,000 and 77,000 mg/kg, respectively). However, high amounts of Ca (1030 mg/kg), and significant contents of Si (204 mg/kg), K (120 mg/kg), Al (100 mg/kg) and Fe (94 mg/kg) were also detected. Finally, moderate amounts of Mn (36 mg/kg), Zn (18 mg/kg) and Ni (11 mg/kg) were found, with minor Sr (7.2 mg/kg), P (7.2 mg/kg), Ti (5.3 mg/kg), As (3 mg/kg) and Co (0.5 mg/kg).

Of considerable importance are the concentrations of radioactive elements that emerged from the results of the radioanalytical methods (Table 4). The concentration of ^{210}Po is surprisingly very high, with an average value of 5.59 Bq g^{-1}, while the concentration of ^{228}Th shows lower values (0.124 Bq g^{-1}). In fact, the ^{210}Po concentration in surface soils with a normal radiation background is in the range of 0.01–0.2 Bq g^{-1} in the absence of anthropogenic influences. A wide variation in ^{210}Po content could depend on the uranium concentration in the bedrock, soil properties, depth of sampling and climatic conditions (Meli et al., 2013a; Carvalho et al., 2017).

4. Discussion

As demonstrated by the wide literature on carcinogenic and supposed carcinogenic fibrous minerals in recent decades, the processes that take place between the inhalation of mineral particles and the development of related diseases are not fully understood (e.g., Asgharian et al., 2018; Gualtieri et al., 2018b; Pacella et al., 2018). Biopersistent fibres in the lungs or cellular environments are mainly considered because fibres that are rapidly dissolved or have a low biopersistence are assumed to have low toxicity and pathogenic potential (Gualtieri et al., 2017; Gualtieri, 2018). Health effects may become evident only after long-term exposure to dust and include pneumoconiosis, hard metal lung disease, systemic poisoning, cancer, irritation and inflammatory lung injuries, allergic responses and others (e.g., World Health Organization, 1999; Aust et al., 2011; Gualtieri, 2017). On the other

Table 4
^{210}Po, ^{238}U, ^{232}Th and ^{228}Th concentration (Bq g^{-1}) of MP epsomite fibres.

Epsomite (MP)	^{210}Po Bq g^{-1}	^{238}U Bq g^{-1}	^{232}Th Bq g^{-1}	^{228}Th Bq g^{-1}	^{228}Th/^{232}Th
1	5.82 ± 0.87	–	–	0.134 ± 0.020	–
2	6.41 ± 0.96	–	–	0.128 ± 0.019	–
3	3.97 ± 0.60	–	–	0.110 ± 0.017	–
4	6.15 ± 0.92	–	–	–	–
Average	**5.59**	**< 1.0 10^{-2}**	**< 1.0 10^{-3}**	**0.124**	**> 124**
σ	1.11	–	–	0.012	–

hand, we did not find studies related to health effects resulting from exposure to water-soluble minerals: we only found studies related to soluble metals and the organic fraction of fine particles. Recently, attention has been gained by the water-soluble fraction of PM, especially because it represents a significant portion of the total mass of PM (Kumagai et al., 2009; Gioda et al., 2011; Ventura et al., 2017). In the toxicological study by Adamson et al. (1999), the authors suggest that the pulmonary response and cell injury following exposure to urban dust could be related to the soluble fraction of particles, probably metal ions, rather than to the number or composition of the insoluble particles. Moreover, the same authors affirm that this fraction, more easily absorbed by the human body, is the most harmful due to its potential toxicity. Other authors suggest that the adverse health effects due to exposure to particle-bound metals are mainly due to the soluble fraction that makes them bioavailable (Salma, 2009; Mugica-Álvarez et al., 2012). Soluble particles, especially those with a very small size, could play an important role in pulmonary toxicity. In addition, soluble carcinogens may pose a risk to the lungs and other organs (World Health Organization, 1999; Adamson et al., 1999). In fact, the solubilised components could spread in biological fluids and react with cells and tissue or reach blood and lymph capillaries, and then easily move to other sites in the human body (Nemmar et al., 2002; Möller et al., 2008). Similarly, the consequent free nanoparticles (e.g., metal oxides) that remain after the dissolution of the fibres in the lungs could migrate to other areas due to the fast exchange mechanisms with blood, especially in the alveolus (Trojan horse effect; Studer et al., 2010; Giordani et al., 2019). Small particles containing iron, such as oxides (e.g., goethite and hematite), hydrate sulphate (jarosite), clays (nontronite) and the thin coating of iron-bearing silicates, were detected on fibrous zeolites using SEM, micro-Raman spectroscopy and transmission electron microscopy (Wise and Tschernich, 1976; Cametti et al., 2013; Croce et al., 2015; Gualtieri et al., 2016). Therefore, the particle-bound insoluble fraction and toxic trace elements could be released in the respiratory system (after the soluble fraction is dissolved) and could play a significant role in disease pathways (Roselli et al., 2015; Bloise et al., 2016; Mattioli et al., 2016b). Moreover, recent studies show that deposited particles directly translocate from the nasal region to the central nervous system via the olfactory bulb and cause brain lesions and other diseases (Oberdörster et al., 2005; Maher et al., 2016; Fang et al., 2017).

As previously described, in the investigated epsomite sample, a considerable number of fibres are of inhalable size (length >5 μm and diameter <3 μm) and thus are potentially able to penetrate into the lungs. Moreover, according to their D_{ae}, the MP fibres can easily penetrate and be deposited in the laryngeal and bronchial respiratory tract. So, if we consider that (i) epsomite is stable in a small range of temperatures and relative humidities (e.g., at 25 °C it is stable at a relative humidity between 50% and 90%), (ii) its stability field rapidly decreases at higher temperatures (Chou and Seal, 2003; Chipera and Vaniman, 2007), and (iii) the pulmonary environmental conditions are a relative humidity of 100% and a temperature of 37 °C, it is likely that inhaled epsomite fibres and particles become a solution phase very rapidly, like a saline spray. In light of this, due to the chemical composition of epsomite crystals, some consideration of their constituents is needed.

Magnesium, the second most abundant cation in cellular systems, and its role in biological systems have been extensively investigated. However, many questions are still awaiting answers and some conflicting results were found (Tam et al., 2003). Magnesium plays an important role in different aspects of immune response, both in animal models and in human systems (Malpuech-Brugere et al., 1998; Petrault et al., 2002; Laires and Monteiro, 2008). Magnesium is involved in thymocyte gene expression, apoptosis and inflammation, and in histological and cytological effects in animal models; it is related to the immune system in athletes, asthma, aging processes and cell apoptosis in humans (Pedersen et al., 1999; Black et al., 2001; Tam et al., 2003; Gombart et al., 2020; Schuh et al., 2020).

Sulphur is the third most abundant mineral based on the percentage of total body weight. The role of elemental sulphur in humans is debated, but it is known that it is an essential element, especially concerning sulphur compounds such as sulphur-containing amino acids (SAAs) and methylsulfonylmethane (MSM), which are often used in medicine (Parcell, 2002). Moreover, some natural sulphur-containing compounds seem to be potent agents for cancer chemoprevention and have anticancer properties (Wu et al., 2005; Nagini, 2008). However, sulphur and a minor amount of other elements were detected in the particles and nanoparticles of photocopiers. Some authors suggest a link between these particles and health issues, but further investigation is needed (Barthel et al., 2011; Bello et al., 2013).

Although epsomite and magnesium sulphate have numerous medical and pharmaceutical applications, *in-vitro* and *in-vivo* studies on magnesium sulphate show controversial or unclear results. $MgSO_4$ is used as an anticonvulsant or tocolytic agent in pregnancy (Ueshima et al., 2003) and could affect the function of the heart (Wright et al., 1996), lungs (Kumasaka et al., 1996), brain (Browne et al., 2004) and central nervous system (Chen et al., 2005). Other studies demonstrate a neuroprotective effect in the foetus (Rouse et al., 2008; Conde-Agudelo and Romero, 2009; Doyle et al., 2009) and also strong anti-inflammatory properties and an anti-hyperalgesic effect in *in-vitro* and *in-vivo* studies (Lin et al., 2010; Lee et al., 2011; Tam et al., 2011; Gao et al., 2013; Srebro et al., 2014). However, $MgSO_4$ exposure showed toxic effects like low body weight, delayed differentiation and reversible changes in rib morphology in the offspring of rats (Katsumata et al., 1998) and neurodegeneration after pregnant female subcutaneous administration (Ozdogan et al., 2013). Preliminary results suggest a significant effect of magnesium sulphate on human gastric adenocarcinoma stomach (AGS) cells. It inhibits the viability and proliferation of AGS cells, which regulate the expression and/or release of pro-inflammatory cytokines; this results in cytotoxicity in moderate concentrations and time periods (Zhang et al., 2015). However, other authors did not find a direct relationship between AGS and cell viability and anti-apoptotic effects, and further research is required to determine how caspase activation was inhibited by $MgSO_4$ (Xia et al., 2016).

In addition, studies on the biological effects of inhaled magnesium sulphate whiskers, which are soluble in water, were performed on rats (Adachi et al., 1991; Hori et al., 1994). Magnesium sulphate whiskers are man-made mineral fibres (MMMFs) consisting of magnesium sulphate and magnesium hydroxide ($MgSO_4{\cdot}5\ Mg(OH)_2{\cdot}3H_2O$) that are used to reinforce plastics and rubbers and to thicken paint materials and epoxy adhesives. The results are once again contradictory. In fact, in the study of Adachi et al. (1991), the incidence of tumours was significant, while in the study of Hori et al. (1994), the incidence was not significant compared to control groups.

Due to the scarcity of toxicological data on epsomite in the literature, the health effect of magnesium sulphate and magnesium sulphate whiskers were also discussed for comparison, assuming similar products of dissolution. However, the chemical structures are different, and therefore the related toxic effects could also be different. Regarding small particles (e.g., metals), the Trojan horse-type mechanism remaining after fibre dissolution (as in the case of epsomite) and the possible effects of these particles on human health should not be underestimated. In the long term, probably no traces of the passage of soluble mineral fibres and other soluble materials remain in the lungs, and therefore it is difficult to trace the origin of metal particles that have accumulated in the body. However, it is known that metal nanoparticles may accumulate in organisms, such as in the lymph nodes, and then act as cofactors for chronic inflammation or even malignant transformation, as seen, for example, from environmental pollution (Iannitti et al., 2010). As observed for copper, the physico-chemical parameters of the material and its nature (oxide, ionic, metal) are very important and can cause significantly different *in-vitro* cytotoxicities (Studer et al., 2010). For these reasons, the contribution of particles and nanoparticles that

are detected on the fibre surface of the studied epsomite sample and carried in the lungs could be non-negligible to several illnesses, like other fibrous minerals (Gualtieri et al., 2019). In fact, the chrysotile fibres that are less biopersistent in the lungs compared to other asbestos may be able to quickly release trace metals in the extracellular medium and could play a synergetic factor in the pathogenesis of diseases caused by the inhalation of mineral fibres (Bloise et al., 2016).

In the studied epsomite crystals, a considerable amount of Ca, probably related to gypsum impurities, was detected, coupled with significant Si, K, Al, and Fe (Table 3). Iron and other bioavailable transition metals are known to be very important elements due to their redox properties and they could stimulate the generation of hydroxyl radicals (HO) by Fenton-type reactions, causing extensive oxidative damage (Costa and Dreher, 1997; Roemer et al., 2000; Dominici et al., 2007). Similarly, the other detected trace elements (Mn, Zn, Ni, Sr, P, Ti, As, Co; Table 3), being higher than the baseline values in normal human lung tissues (Vanoeteren et al., 1986), could also play a role in the toxicity pathway in the lungs and other biological systems, losing track of the initial passage in the lungs. Such potentially toxic elements have already been found in asbestos fibres, which play an important role in the pathogenesis of human lung cancer (Dixon et al., 1970; Nemery, 1990; Wei et al., 2014; Bloise et al., 2016, 2020). In the case of biopersistent fibres, the amounts of potentially toxic elements are generally higher than those detected in the studied epsomite fibres (e.g., As 1.5–7 ppm, Co 2–22 ppm, Ni 4–308 ppm, Sr 10–200 ppm; Bloise et al., 2016, 2020). However, epsomite fibres undergo a very fast dissolution and release their cargo of toxic elements into the lung environment in a very short period, thus becoming more dangerous than biopersistent fibres. If these trace elements rapidly accumulate in sufficient amounts in the lungs, via fibre dissolution, they may cause mesothelioma and bronchogenic carcinoma (Dixon et al., 1970; Nemery, 1990; Wei et al., 2014). Thus, we need to consider these mechanisms as possible bioaccumulators of particles and toxic elements over time at different sites in the human body. However, the potential toxic effect of the released major and minor elements and the related toxic concentration level are still open to debate, as suggested for Mg by Gualtieri et al. (2019).

Of great interest in the investigated epsomite sample are the surprisingly high amounts of radioactive element concentrations, especially for ^{210}Po. Naturally occurring ^{210}Po and its grandparent ^{210}Pb are members of the ^{238}U decay series. ^{210}Po is an alpha radioactive emitter with a half-life of approximately 138 days, and it decays to stable Pb (Meli et al., 2013b; Carvalho et al., 2017); it is the only naturally occurring radioactive isotope of polonium with a half-life long enough to play a significant role in environmental processes (World Health Organization, 1999). However, the behaviour of ^{210}Po in aqueous systems is generally dominated by adsorption onto surfaces, although incorporation into colloids, biovolatilisation and precipitation in sulphides can be important in some circumstances (World Health Organization, 1999). In acidic solutions, trace polonium is precipitated by hydrogen sulphide (H_2S) and other insoluble sulphides. Moreover, polonium has a high affinity for particles (Seiler et al., 2011). Therefore, the concentration of dissolved polonium can be strictly controlled by sulphur recycling, in which the dissolution and reprecipitation of sulphur minerals occur (Seiler et al., 2011; World Health Organization, 1999).

Although we still do not know if these elements are present in the epsomite structure as a substitute for Mg or as impurities, it is evident that ^{210}Po and ^{228}Th may be vehiculated inside the lungs during inhalation. Radioactive particles that are inhaled and deposited in the lungs cause an irradiation of bronchial/alveolar tissues, and this could result in a malignant cellular transformation and the development of lung cancer (Sturm, 2011). Moreover, radionuclides can also be carried away from the lungs and damage other parts of the body (World Health Organization, 1999). Regarding internally deposited radionuclides, IARC (2001) determine that the epidemiological studies of nuclear industry workers exposed to ^{210}Po are inadequate for drawing a conclusion about cancer risk. Moreover, very few data exist concerning the human toxicity of polonium (Ansoborlo et al., 2012) and the possibility of being exposed to it in the environment (Lee et al., 2009). Seiler and Wiemels (2012) stated that many biological and toxicological studies on ^{210}Po are many decades old and that to assess environmentally relevant exposure to ^{210}Po and its capacity to kill or damage critical reproductive, embryonic or hematopoietic cells in humans, new studies (with modern tools) are needed.

The very harmful effect of radioactive elements on human health is well known, but information on human exposure pathways is essential for the identification of the real health impact. An exposure pathway (i.e., the means by which hazardous materials move through the environment from a source to a point of contact with people) generally includes (1) a source of contamination; (2) a mechanism to transport a material from the source to the air, water or soil; (3) a point where people come into contact with contaminated air, water or soil; and (4) a route of entry into the body (eating or drinking contaminated materials, breathing contaminated air, or absorbing contaminants through the skin). In the case of the studied epsomite, the source of contamination is represented by the toxic chemical and radioactive elements contained in the fibres, and the industrial processes associated with the commercial operation included mining, milling, screening and processing. This took place extensively in the past and resulted in high occupational exposure to epsomite fibres. Although the mine is inactive today, the widespread presence of epsomite in the area could still potentially expose anyone crossing the surrounding area. The main route of entry into the body of these fibres is the breathing of contaminated air, which is facilitated by the remarkable volatility of the fibres and their morphology and solubility. However, if we consider that the entire mining area is affected by the presence of both surface and ground waters, potential exposure due to drinking contaminated water cannot be excluded, especially in the case of highly soluble minerals such as epsomite. Noteworthy, Dinelli (1995) found a high presence of dissolved $MgSO_4$ in the stream waters that interacted with the Boratella mine dump, another sulphur mine located ~12 km NW from Perticara with which shares similar geological features. Additionally, despite the fact that the studied epsomite fibres were found in an abandoned mine, it must be taken into account that the same mineral can be largely present in other environments, such as buildings, in the form of saline efflorescence. Epsomite and other highly soluble materials, including several minerals commonly used in many industries, are numerous, and the lung burden may be more significant than expected, especially for occupationally and environmentally exposed people. Perhaps the load from the airways could be greater than is usually assumed. Certainly, a complete reconstruction of the different pathways of environmental epsomite exposure could be a key aim of ongoing research, and an evaluation of the real exposure of humans to ^{210}Po and ^{228}Th vehiculated by epsomite fibres is needed. Finally, another question that remains open is the presence of high quantities of radioactive elements in the studied epsomite fibres. It is important to understand if this radioactive anomaly is related to local factors (and what they are) or if epsomite could be a mineral particularly available to host radioactive elements such as ^{210}Po and ^{228}Th. The latter case would make epsomite a mineral to be carefully monitored in all other contexts in which it can be found worldwide.

Due to their high solubility in water, the potential toxicity of the studied epsomite fibres derives from the chemical composition (major and minor elements) rather than the fibrous habit and size parametres. In the case of epsomite, the particular fibrous morphology is only the medium that allows the mineral to reach the innermost respiratory areas, but the real element of risk is the chemicals originating from mineral particles during dissolution. Due to the lack of *in-vitro*, *in-vivo* and epidemiological studies, the identified hazard of epsomite for humans is theoretical, and further detailed studies are needed for a full assessment of its eventual toxicity.

5. Conclusions

In this work, we characterise the fibrous mineral epsomite from Perticara Mine (Central Italy) and discuss its possible toxicological role in human health. Morphology and morphometry investigations highlight the presence of significant amounts of small fibres, which are potentially inhalable for humans. About 25% of the measured fibres are thinner or equal to 3 μm and almost every fibre is longer than 5 μm, so there is a significant fraction that is able to penetrate the lungs. Due to the instability of epsomite at lung conditions (37 °C and 100% relative humidity), the inhaled fibres rapidly become a solution. Chemical analysis on epsomite crystals revealed the presence of toxic elements (As, Co, Fe, Mn, Ni, Sr, Ti, Zn) and very high amounts of radioactive isotopes (^{210}Po and ^{228}Th). Consequently, the entire load of hazardous elements could be quickly released into the lung environment and thus have an effect on human health.

Considering that natural epsomite is common in several natural and anthropic environments worldwide (e.g., caves, mines, geological outcrops, mineral springs, efflorescence) and also has several applications, the presence of toxic elements and radioactive isotopes in the studied epsomite fibres suggests the need for attention in handling other epsomite samples. Investigations on other commonly used soluble minerals could also be important in assessing the eventual exposure of humans to hazardous materials.

Although toxicity is generally evaluated only for biopersistent minerals, our findings suggest that soluble phases should also be investigated and their possible hazard assessed.

The natural epsomite, which is highly soluble in the lung environment, can be considered a representative case study to investigate this interaction. These preliminary results can be the basis for further detailed studies on the content of hazardous elements in building materials and the interaction of toxic elements (e.g., metals or radioactive particles) with humans and their eventual harmful effects on health.

Funding

This research was conducted under the project “Fibers a Multidisciplinary Mineralogical, Crystal-Chemical and Biological Project to Amend the Paradigm of Toxicity and Cancerogenicity of Mineral Fibers” (PRIN: PROGETTI DI RICERCA DI RILEVANTE INTERESSE NAZIONALE—Bando, 2017—Prot. 20173X8WA4).

Declaration of competing interest

The authors declare that they have no known competing financial interests or personal relationships that could have appeared to influence the work reported in this paper.

Acknowledgements

Thanks to Dr. Georgia Cametti (University of Bern, CH) for the important suggestions, for attempts to refine the crystal structure with Single Crystal X Ray Diffraction and for the revision of the manuscript. Thanks are due to “Museo Sulphur” of Perticara (RN) for kind hospitality to the author (MG) and logistic support during the sampling phase. Thanks to Federazione Speleologica Regionale dell’Emilia Romagna (FSRER) for having promoted the re-exploration of the Perticara mine (Project: Gessi e Solfi della Romagna Orientale), within which this study was developed. Authors are very grateful to the three anonymous reviewers for their detailed reviews of this manuscript, improving it by means of several comments and suggestions. Editorial assistance provided by José L. Domingo was greatly appreciated.

Appendix A. Supplementary data

Supplementary data to this article can be found online at https://doi.org/10.1016/j.envres.2021.112579.

References

Adachi, S., Takemoto, K., Kimura, K., 1991. Tumorigenicity of fine man-made fibers after intratracheal administrations to hamsters. Environ. Res. 54 (1), 52–73. https://doi.org/10.1016/S0013-9351(05)80194-X.

Adamson, I.Y., Prieditis, H., Vincent, R., 1999. Pulmonary toxicity of an atmospheric particulate sample is due to the soluble fraction. Toxicol. Appl. Pharmacol. 157 (1), 43–50. https://doi.org/10.1006/taap.1999.8658.

Andujar, P., Lacourt, A., Brochard, P., Pairon, J.C., Jaurand, M.C., Jean, D., 2016. Five years update on relationships between malignant pleural mesothelioma and exposure to asbestos and other elongated mineral particles. J. Toxicol. Environ. Health, Part B 19, 151–172. https://doi.org/10.1080/10937404.2016.1193361.

Ansoborlo, E., Berard, P., Den Auwer, C., Leggett, R., Menetrier, F., Younes, A., Montavon, G., Moisy, P., 2012. Review of chemical and radiotoxicological properties of polonium for internal contamination purposes. Chem. Res. Toxicol. 25 (8), 1551–1564. https://doi.org/10.1021/tx300072w.

Anthony, J.W., Bideaux, R.A., Bladh, K.W., Nichols, M.C., 1990. Elements, sulfides. Sulfosalts 1 (of Handbook of Mineralogy. Tucson, Arizona, USA. Mineral Data Publishing).

Asgharian, B., Owen, T.P., Kuempel, E.D., Jarabek, A.M., 2018. Dosimetry of inhaled elongate mineral particles in the respiratory tract: the impact of shape factor. Toxicol. Appl. Pharmacol. 361, 27–35. https://doi.org/10.1016/j.taap.2018.05.001.

Aust, A.E., Cook, P.M., Dodson, R.D., 2011. Morphological and chemical mechanisms of elongated mineral particle toxicities. J. Toxicol. Environ. Health, Part B 14, 40–75. https://doi.org/10.1080/10937404.2011.556046.

Ballirano, P., Pacella, A., Cremisini, C., Nardi, E., Fantauzzi, M., Atzei, D., Rossi, A., Cametti, G., 2015. Fe (II) segregation at a specific crystallographic site of fibrous erionite: a first step toward the understanding of the mechanisms inducing its carcinogenicity. Microporous Mesoporous Mater. 211, 49–63. https://doi.org/10.1016/j.micromeso.2015.02.046.

Barthel, M., Pedan, V., Hahn, O., Rothhardt, M., Bresch, H., Jann, O., Seeger, S., 2011. XRF-analysis of fine and ultrafine particles emitted from laser printing devices. Environ. Sci. Technol. 45 (18), 7819–7825. https://doi.org/10.1021/es201590q.

Bello, D., Martin, J., Santeufemio, C., Sun, Q., Lee Bunker, K., Shafer, M., Demokritou, P., 2013. Physicochemical and morphological characterisation of nanoparticles from photocopiers: implications for environmental health. Nanotoxicology 7 (5), 989–1003. https://doi.org/10.3109/17435390.2012.689883.

Biagioni, C., Mauro, D., Pasero, M., 2020. Sulfates from the pyrite ore deposits of the Apuan Alps (Tuscany, Italy): a review. Minerals 10 (12), 1092. https://doi.org/10.3390/min10121092.

Black, S., Yu, H., Lee, J., Sachchithananthan, M., Medcalf, R.L., 2001. Physiologic concentrations of magnesium and placental apoptosis: prevention by antioxidants. Obstet. Gynecol. 98 (2), 319–324. https://doi.org/10.1016/S0029-7844(01)01418–1.

Bloise, A., Barca, D., Gualtieri, A.F., Pollastri, S., Belluso, E., 2016. Trace elements in hazardous mineral fibres. Environ. Pollut. 216, 314–323. https://doi.org/10.1016/j.envpol.2016.06.007.

Bloise, A., Ricchiuti, C., Punturo, R., Pereira, D., 2020. Potentially toxic elements (PTEs) associated with asbestos chrysotile, tremolite and actinolite in the Calabria region (Italy). Chemical Geology, 558, p.119896. https://doi.org/10.1016/j.chemgeo.2020.119896.

Boulanger, G., Andujar, P., Pairon, J.C., Billon-Galland, M.A., Dion, C., Dumortier, P., Brochard, P., Sobaszek, A., Bartsch, P., Paris, C., Jaurand, M.C., 2014. Quantification of short and long asbestos fibers to assess asbestos exposure: a review of fiber size toxicity. Environ. Health 13 (1), 1–18. https://doi.org/10.1186/1476-069X-13-59.

Brown, J.S., Gordon, T., Price, O., Asgharian, B., 2013. Thoracic and respirable particle definitions for human health risk assessment. Part. Fibre Toxicol. 10 (1), 1–12. https://doi.org/10.1186/1743-8977-10-12.

Browne, K.D., Leoni, M.J., Iwata, A., Smith, D.H., 2004. Acute treatment with $MgSO_4$ attenuates long-term hippocampal tissue loss after brain trauma in the rat. J. Neurosci. Res. 77 (6), 878–883. https://doi.org/10.1002/jnr.20215.

Cametti, G., Pacella, A., Mura, F., Rossi, M., Ballirano, P., 2013. New morphological, chemical, and structural data of woolly erionite-Na from Durkee, Oregon, USA. Am. Mineral. 98, 2155–2163. https://doi.org/10.2138/am.2013.4474.

Cangiotti, M., Battistelli, M., Salucci, S., Falcieri, E., Mattioli, M., Giordani, M., Ottaviani, M.F., 2017. Electron paramagnetic resonance and transmission electron microscopy study of the interactions between asbestiform zeolite fibers and model membranes. J. Toxicol. Environ. Health, Part A 80 (3), 171–187. https://doi.org/10.1080/15287394.2016.1275901.

Cangiotti, M., Salucci, S., Battistelli, M., Falcieri, E., Mattioli, M., Giordani, M., Ottaviani, M.F., 2018. EPR, TEM and cell viability study of asbestiform zeolite fibers in cell media. Colloids Surf. B Biointerfaces 161, 147–155. https://doi.org/10.1016/j.colsurfb.2017.10.045.

Cardile, V., Lombardo, L., Belluso, E., Panico, A., Capella, S., Balazy, M., 2007. Toxicity and carcinogenicity mechanisms of fibrous antigorite. Int. J. Environ. Res. Publ. Health 4 (1), 1–9. https://doi.org/10.3390/ijerph2007010001.

Carvalho, F., Fernandes, S., Fesenko, S., Holm, E., Howard, B., Martin, P., Phaneuf, M., Porcelli, D., Pröhl, G., Twining, J., 2017. The environmental behaviour of polonium. Int. Atomic Energy Agency 484.

Chen, H.H., Wei, C.T., Lin, Y.R., 2005. Neonatal toluene exposure alters agonist and antagonist sensitivity and NR2B subunit expression of NMDA receptors in cultured cerebellar granule neurons. Toxicol. Sci. 85 (1), 666–674. https://doi.org/10.1093/toxsci/kfi100.

Chipera, S.J., Vaniman, D.T., 2007. Experimental stability of magnesium sulfate hydrates that may be present on Mars. Geochem. Cosmochim. Acta 71 (1), 241–250. https://doi.org/10.1016/j.gca.2006.07.044.

Chou, I.M., Seal, R.R., 2003. Determination of epsomite-hexahydrite equilibria by the humidity-buffer technique at 0.1 MPa with implications for phase equilibria in the system $MgSO_4$-H_2O. Astrobiology 3 (3), 619–630. https://doi.org/10.1089/153110703322610708.

Conde-Agudelo, A., Romero, R., 2009. Antenatal magnesium sulfate for the prevention of cerebral palsy in preterm infants less than 34 weeks' gestation: a systematic review and metaanalysis. Am. J. Obstet. Gynecol. 200 (6), 595–609. https://doi.org/10.1016/j.ajog.2009.04.005.

Conti, P., Cornamusini, G., Carmignani, L., 2020. An outline of the geology of the Northern Apennines (Italy), with geological map at 1:250,000 scale. Italian J. Geosci. 139 (2), 149–194. https://doi.org/10.3301/IJG.2019.25.

Costa, D.L., Dreher, K.L., 1997. Bioavailable transition metals in particulate matter mediate cardiopulmonary injury in healthy and compromised animal models. Environ. health Perspect. 105 (5), 1053–1060. https://doi.org/10.1289/ehp.97105s51053.

Croce, A., Allegrina, M., Rinaudo, C., Gaudino, G., Yang, H., Carbone, M., 2015. Numerous iron-rich particles lie on the surface of erionite fibers from Rome (Oregon, USA) and Karlik (Cappadocia, Turkey). Microsc. Microanal. 21 (5), 1341–1347. https://doi.org/10.1017/S1431927615014762.

Crovella, S., Bianco, A.M., Vuch, J., Zupin, L., Moura, R.R., Trevisan, E., Schneider, M., Brollo, A., Nicastro, E.M., Cosenzi, A., Zabucchi, G., 2016. Iron signature in asbestos-induced malignant pleural mesothelioma: a population-based autopsy study. J. Toxicol. Environ. Health, Part A 79 (3), 129–141. https://doi.org/10.1080/15287394.2015.1123452.

Del Rio-Salas, R., Ayala-Ramìrez, Y., Loredo-Portales, R., Romero, F., Molina-Freaner, F., Minjarez-Osorio, C., Pi-Puig, T., Ochoa-Landìn, L., Moreno-Rodrìguez, V., 2019. Mineralogy and geochemistry of rural road dust and nearby mine tailings: a case of ignored pollution hazard from an abandoned mining site in semi-arid zone. Nat. Resour. Res. 28 (4). https://doi.org/10.1007/s11053-019-09472-x.

Di Giuseppe, D., 2020. Characterization of Fibrous Mordenite: A First Step for the Evaluation of its Potential Toxicity. Crystals, 10, vol. 9 769 https://doi.org/10.3390/cryst10090769.

Dinelli, E., 1995. Stream sediments and stream waters as tracers of the environmental impact of sulphur mine wastes (Savio valley, Romagna-Marche Apennines, Northern-central Italy). Mineral. Petrogr. Acta XXXVIII, 89–112.

Dixon, J.R., Lowe, D.B., Richards, D.E., Cralley, L.J., Stokinger, H.E., 1970. The role of trace metals in chemical carcinogenesis: asbestos cancers. Cancer Res. 30, 1068–1074.

Dominici, F., Peng, R.D., Ebisu, K., Zeger, S.L., Samet, J.M., Bell, M.L., 2007. Does the effect of PM_{10} on mortality depend on PM nickel and vanadium content? A reanalysis of the NMMAPS data. Environ. health Perspect. 115 (12), 1701–1703. https://doi.org/10.1289/ehp.10737.

Doyle, L.W., Crowther, C.A., Middleton, P., Marret, S., Rouse, D., 2009. Magnesium sulphate for women at risk of preterm birth for neuroprotection of the fetus. Cochrane Database of Systematic Reviews, (1). Art. No.: CD004661. https://doi.org/10.1002/14651858.CD004661.pub3.

European Committee for Standardization (CEN), 1993. Workplace Atmospheres – Size Fraction Definitions for Measurement of Airborne Particles. Report BS EN 481. British Standards Institute, London.

EPA Environmental Protection Agency Air Quality Criteria for Particulate Matter, 1996. EPA/600/P-95/001CF. National Center for Environmental Assessment, Research Triangle Park, NC. vol. III.

Fang, T., Zeng, L., Gao, D., Verma, V., Stefaniak, A.B., Weber, R.J., 2017. Ambient size distributions and lung deposition of aerosol dithiothreitol-measured oxidative potential: contrast between soluble and insoluble particles. Environ. Sci. Technol. 51 (12), 6802–6811. https://doi.org/10.1021/acs.est.7b01536.

Fubini, B., 2001. The Physical and Chemical Properties of Asbestos Fibres Which Contribute to Biological Activity. Asbestos Health Effect Conference, May 24–25. US Environmental Protection Agency, Oakland, CA.

Gao, F., Ding, B.Z., Zhou, L.G., Xu, H., 2013. Magnesium sulfate provides neuroprotection in lipopolysaccharide-activated primary microglia by inhibiting NF-kB pathway. J. Surg. Res. 184 (2), 944–950. https://doi.org/10.1016/j.jss.2013.03.034.

García-Romero, E., Suárez, M., 2013. Sepiolite-palygorskite: textural study and genetic considerations. Appl. Clay Sci. 86, 129–144. https://doi.org/10.1016/j.clay.2013.09.013.

Gianfagna, A., Ballirano, P., Bellatreccia, F., Bruni, B., Paoletti, L., Oberti, R., 2003. Characterization of amphibole fibres linked to mesothelioma in the area of Biancavilla, Eastern Sicily, Italy. Mineral. Mag. 67 (6), 1221–1229. https://doi.org/10.1180/0026461036760160.

Gioda, A., Amaral, B.S., Monteiro, I.L.G., Saint'Pierre, T.D., 2011. Chemical composition, sources, solubility, and transport of aerosol trace elements in a tropical region. J. Environ. Monit. 13 (8), 2134–2142. https://doi.org/10.1039/C1EM10240K.

Giordani, M., Mattioli, M., Dogan, M., Dogan, A.U., 2016. Potential carcinogenic erionite from Lessini Mounts, NE Italy: morphological, mineralogical and chemical characterization. J. Toxicol. Environ. Health, Part A 79 (18), 808–824. https://doi.org/10.1080/15287394.2016.1182453.

Giordani, M., Mattioli, M., Ballirano, P., Pacella, A., Cenni, M., Boscardin, M., Valentini, L., 2017. Geological occurrence, mineralogical characterization, and risk assessment of potentially carcinogenic erionite in Italy. J. Toxicol. Environ. Health, Part B 20 (2), 81–103. https://doi.org/10.1080/10937404.2016.1263586.

Giordani, M., Cametti, G., Di Lorenzo, F., Churakov, S.V., 2019. Real-time observation of fibrous zeolites reactivity in contact with simulated lung fluids (SLFs) obtained by atomic force microscope (AFM). Minerals 9 (2), 83. https://doi.org/10.3390/min9020083.

Giordani, M., Mattioli, M., Cangiotti, M., Fattori, A., Ottaviani, M.F., Betti, M., Ballirano, P., Pacella, A., Di Giuseppe, D., Scognamiglio, V., Hanuskova, M., Gualtieri, A.F., 2021. Characterisation of potentially toxic natural fibrous zeolites by means of electron paramagnetic resonance spectroscopy and morphological-mineralogical studies. Press. https://doi.org/10.1016/j.chemosphere.2021.133067.

Gombart, A.F., Pierre, A., Maggini, S., 2020. A review of micronutrients and the immune system–working in harmony to reduce the risk of infection. Nutrients 12 (1), 236. https://doi.org/10.3390/nu12010236.

Gonda, I., 1985. Abd El Khalik, A.F On the calculation of aerodynamic diameters of fibers. Aerosol. Sci. Technol. 4 (2), 233–238. https://doi.org/10.1080/02786828508959051.

Groppo, C., Tomatis, M., Turci, F., Gazzano, E., Ghigo, D., Compagnoni, R., Fubini, B., 2005. Potential toxicity of nonregulated asbestiform minerals: balangeroite from the western Alps. Part 1: identification and characterization. J. Toxicol. Environ. Health, Part A 68 (1), 1–19. https://doi.org/10.1080/15287390590523867.

Gualtieri, A.F., Gandolfi, N.B., Pollastri, S., Pollok, K., Langenhorst, F., 2016. Where is iron in erionite? A multidisciplinary study on fibrous erionite-Na from Jersey (Nevada, USA). Sci. Rep. 6 (1), 1–11. https://doi.org/10.1038/srep37981.

Gualtieri, A.F., Mossman, B.T., Roggli, V.L., 2017. Towards a general model to predict the toxicity and pathogenicity of mineral fibres. In: Mineral Fibres: Crystal Chemistry, Chemical-Physical Properties, Biological Interaction and Toxicity: European Mineralogical Union–EMU Notes in Mineralogy, vol. 18. pp. 501–532 (Chapter 15).

Gualtieri, A.F., Gandolfi, N.B., Passaglia, E., Pollastri, S., Mattioli, M., Giordani, M., Ottaviani, M.F., Cangiotti, M., Bloise, A., Barca, D., Vigliaturo, R., 2018a. Is fibrous ferrierite a potential health hazard? Characterization and comparison with fibrous erionite. Am. Mineral.: J. Earth Planet. Mater. 103 (7), 1044–1055. https://doi.org/10.2138/am-2018-6508.

Gualtieri, A.F., Pollastri, S., Gandolfi, N.B., Gualtieri, M.L., 2018b. In vitro acellular dissolution of mineral fibres: a comparative study. Sci. Rep. 8 (1), 1–12. https://doi.org/10.1038/s41598-018-25531-4.

Gualtieri, A.F., Lusvardi, G., Zoboli, A., Di Giuseppe, D., Gualtieri, M.L., 2019. Biodurability and release of metals during the dissolution of chrysotile, crocidolite and fibrous erionite. Environ. Res. 171, 550–557. https://doi.org/10.1016/j.envres.2019.01.011.

Gualtieri, A.F., 2017. Mineral fibres: crystal chemistry, chemical-physical properties. Biol. Interaction Toxicity 18, of EMU Notes in Mineralogy. London, UK. European Mineralogical Union and the Mineralogical Society of Great Britain and Ireland.

Gualtieri, A.F., 2018. Towards a quantitative model to predict the toxicity/pathogenicity potential of mineral fibers. Toxicol. Appl. Pharmacol. 361, 89–98. https://doi.org/10.1016/j.taap.2018.05.012.

Hesterberg, T.W., Chase, G., Axten, C., Miller, W.C., Musselman, R.P., Kamstrup, O., Hadley, J., Morscheidt, C., Bernstein, D.M., Thevenaz, P., 1998. Biopersistence of synthetic vitreous fibers and amosite asbestos in the rat lung following inhalation. Toxicol. Appl. Pharmacol. 151 (2), 262–275. https://doi.org/10.1006/taap.1998.8472.

Heyder, J., Gebhart, J., Rudolf, G., Schiller, C.F., Stahlhofen, W., 1986. Deposition of particles in the human respiratory tract in the size range 0.005–15 μm. J. Aerosol Sci. 17 (5), 811–825. https://doi.org/10.1016/0021-8502(86)90035-2.

Hochella, M.F., 1993. Surface chemistry, structure, and reactivity of hazardous mineral dust. In: Guthrie, G.D., Mossman, B.T. (Eds.), Health Effects of Mineral Dusts. Bookcrafters. Reviews in Mineralogy, 28, Chelsea, MI, pp. 275–308. https://doi.org/10.1515/9781501509711-011.

Hori, H., Kasai, T., Haratake, J., Ishimatsu, S., Oyabu, T., Yamato, H., Higashi, T., Tanaka, I., 1994. Biological effects of inhaled magnesium sulphate whiskers in rats. Occup. Environ. Med. 51 (7), 492–499. https://doi.org/10.1136/oem.51.7.492.

Iannitti, T., Capone, S., Gatti, A., Capitani, F., Cetta, F., Palmieri, B., 2010. Intracellular heavy metal nanoparticle storage: progressive accumulation within lymph nodes with transformation from chronic inflammation to malignancy. Int. J. Nanomed. 5 (955). https://doi.org/10.2147/IJN.S14363.

IARC, 2001. Monographs Evaluat. Carcinogenic Risk. Human 78, Ionizing Radiation, Part 2: Some Internally Deposited Radionuclides, World Health Organization, IARC Press, Lyon, France.

Katsumata, Y., Inoue, K., Shimamura, K.Y., 1998. A study for effects on pre- and postnatal development, including maternal function in rats treated subcutaneously with magnesium sulfate. J. Toxicol. Sci. 23, 67–79. https://doi.org/10.2131/jts.23.SupplementI_67.

Kumagai, K., Iijima, A., Tago, H., Tomioka, A., Kozawa, K., Sakamoto, K., 2009. Seasonal characteristics of water-soluble organic carbon in atmospheric particles in the inland Kanto plain. Japan Atmos. Environ. 43 (21), 3345–3351. https://doi.org/10.1016/j.atmosenv.2009.04.008.

Kumasaka, D., Lindeman, K.S., Clancy, J., Lande, B., Croxton, T.L., Hirshman, C.A., 1996. MgSO4 relaxes porcine airway smooth muscle by reducing Ca^{2+} entry. Am. J. Physiol. Lung Cell Mol. Physiol. 270 (3), L469–L474. https://doi.org/10.1152/ajplung.1996.270.3.L469.

Laires, M.J., Monteiro, C., 2008. Exercise, Magnesium and Immune Function. Magnesium Research. p. 21. https://doi.org/10.1684/mrh.2008.0136.

Larson, D., Powers, A., Ambrosi, J.P., Tanji, M., Napolitano, A., Flores, E.G., Baumann, F., Pellegrini, L., Jennings, C.J., Buck, B.J., McLaurin, B.T., 2016. Investigating palygorskite's role in the development of mesothelioma in southern Nevada: insights into fiber-induced carcinogenicity. J. Toxicol. Environ. Health, Part B 19 (5–6), 213–230. https://doi.org/10.1080/10937404.2016.1195321.

Lee, C.W., Kang, M.J., Lee, W., Choi, G.S., Cho, Y.H., Kim, H.R., Chung, K.H., 2009. Assessment of 210 Po in foodstuffs consumed in Korea. J. Radioanal. Nucl. Chem. 279 (2), 519–522. https://doi.org/10.1007/s10967-007-7336-y.

Lee, C.Y., Jan, W.C., Tsai, P.S., Huang, C.J., 2011. Magnesium sulfate mitigates acute lung injury in endotoxemia rats. J. Trauma Acute Care Surgery 70 (5), 1177–1185, 10.1097/TA.0b013e31820ca695.

Lin, C.Y., Tsai, P.S., Hung, Y.C., Huang, C.J., 2010. L-type calcium channels are involved in mediating the anti-inflammatory effects of magnesium sulphate. Br. J. Anaesth. 104 (1), 44–51. https://doi.org/10.1093/bja/aep336.

Maguregui, M., Knuutinen, U., Castro, K., Madariaga, J.M., 2010. Raman spectroscopy as a tool to diagnose the impact and conservation state of Pompeian second and fourth style wall paintings exposed to diverse environments (House of Marcus Lucretius). J. Raman Spectrosc. 41 (11), 1400–1409. https://doi.org/10.1002/jrs.2671.

Maher, B.A., Ahmed, I.A.M., Karloukovski, V., MacLaren, D.A., Foulds, P.G., Allsop, D., Mann, D.M.A., Torres-Jardón, R., Calderon-Garciduenas, L., 2016. Magnetite Pollution Nanoparticles in the Human Brain. Proc. Nat. Acad. Sci. U.S.A vol. 113 (39), 10797. https://doi.org/10.1073/pnas.1605941113.

Malpuech-Brugere, C., Kuryszko, J., Nowacki, W., Rock, E., Rayssiguier, Y., Mazur, A., 1998. Early morphological and immunological alterations in the spleen during magnesium deficiency in the rat. Magnes. Res. 11 (3), 161–169.

Mattioli, M., Giordani, M., Dogan, M., Cangiotti, M., Avella, G., Giorgi, R., Dogan, A.U., Ottaviani, M.F., 2016a. Morpho-chemical characterization and surface properties of carcinogenic zeolite fibers. J. Hazard Mater. 306, 140–148. https://doi.org/10.1016/j.jhazmat.2015.11.015.

Mattioli, M., Giardini, L., Roselli, C., Desideri, D., 2016b. Mineralogical characterization of commercial clays used in cosmetics and possible risk for health. Appl. Clay Sci. 119, 449–454. https://doi.org/10.1016/j.clay.2015.10.023.

Mattioli, M., Giordani, M., Arcangeli, P., Valentini, L., Boscardin, M., Pacella, A., Ballirano, P., 2018. Prismatic to asbestiform offretite from Northern Italy: occurrence, morphology and crystal-chemistry of a new potentially hazardous zeolite. Minerals 8 (2), 69. https://doi.org/10.3390/min8020069.

Maxim, L.D., Hadley, J.G., Potter, R.M., Niebo, R., 2006. The role of fiber durability/biopersistence of silica-based synthetic vitreous fibers and their influence on toxicology. Regul. Toxicol. Pharmacol. 46 (1), 42–62. https://doi.org/10.1016/j.yrtph.2006.05.003.

Meli, M.A., Cantaluppi, C., Desideri, D., Benedetti, C., Feduzi, L., Ceccotto, F., Fasson, A., 2013a. Radioactivity measurements and dosimetric evaluation in meat of wild and bred animals in central Italy. Food Control 30 (1), 272–279. https://doi.org/10.1016/j.foodcont.2012.07.038.

Meli, M.A., Desideri, D., Penna, A., Ricci, F., Penna, N., Roselli, C., 2013b. ^{210}Po and ^{210}Pb concentration in environmental samples of the Adriatic Sea. Int. J. Environ. Res. 7 (1), 51–60. https://doi.org/10.22059/ijer.2012.585.

Meli, M.A., Desideri, D., Fagiolino, I., Roselli, C., 2019. Trace elements, ^{210}Po and ^{210}Pb in a selection of berries on commercial sale in Italy. J. Radioanal. Nucl. Chem. 321 (2), 647–657. https://doi.org/10.1007/s10967-019-06604-8.

Miller, F.J., Gardner, D.E., Graham, J.A., Lee, Jr., R.E., Wilson, W.E., Bachmann, J.D., 1979. Size considerations for establishing a standard for inhalable particles. J. Air Pollut. Control Assoc. 29 (6), 610–615. https://doi.org/10.1080/00022470.1979.10470831.

Möller, W., Felten, K., Sommerer, K., Scheuch, G., Meyer, G., Meyer, P., Haussinger, K., Kreyling, W.G., 2008. Deposition, retention, and translocation of ultrafine particles from the central airways and lung periphery. Am. J. Respir. Crit. Care Med. 177 (4), 426–432. https://doi.org/10.1164/rccm.200602-301OC.

Morillas, H., Maguregui, M., Trebolazabala, J., Madariaga, J.M., 2015. Nature and origin of white efflorescence on bricks, artificial stones, and joint mortars of modern houses evaluated by portable Raman spectroscopy and laboratory analyses. Spectrochim. Acta Mol. Biomol. Spectrosc. 136, 1195–1203. https://doi.org/10.1016/j.saa.2014.10.006.

Mugica-Álvarez, V., Figueroa-Lara, J., Romero-Romo, M., Sepúlveda-Sánchez, J., López-Moreno, T., 2012. Concentrations and properties of airborne particles in the Mexico City subway system. Atmos. Environ. 49, 284–293. https://doi.org/10.1016/j.atmosenv.2011.11.038.

Nagini, S., 2008. Cancer chemoprevention by garlic and its organosulfur compounds-panacea or promise? Anti Cancer Agents Med. Chem. 8 (3), 313–321. https://doi.org/10.2174/187152008783961879.

Navarro, R., Pereira, D., Fernández de Arévalo, E., Sebastián-Pardo, E.M., Rodriguez-Navarro, C., 2021. Weathering of serpentinite stone due to in situ generation of calcium and magnesium sulfates. Construct. Build. Mater. 280 (122402). https://doi.org/10.1016/j.conbuildmat.2021.122402.

Nemery, B., 1990. Metal toxicity and the respiratory tract. Eur. Respir. J. 3, 202–219.

Nemmar, A., Hoet, P.M., Vanquickenborne, B., Dinsdale, D., Thomeer, M., Hoylaerts, M.F., Vanbilloen, H., Mortelmans, L., Nemery, B., 2002. Passage of inhaled particles into the blood circulation in humans. Circulation 105 (4), 411–414. https://doi.org/10.1161/hc0402.104118.

National Institute for Occupational Safety and Health (NIOSH), 2011. Asbestos Fibers and Other Elongate Mineral Particles: State of the Science and Roadmap for Research. Current Intelligence Bulletin 62, Version 4. Department of Health and Human Services: Cincinnati, OH, USA.

Nieva, N.E., Garcia, M.G., Borgnino, L., Borda, L.G., 2021. The role of efflorescent salts associated with sulfide-rich mine wastes in the short-term cycling of arsenic: insights from XRD, XAS, and μ-XRF studies. J. Hazard Mater. 404 (124158). https://doi.org/10.1016/j.jhazmat.2020.124158.

Oberdörster, G., 1988. Lung clearance of inhaled insoluble and soluble particles. J. Aerosol Med. 1 (4), 289–330. https://doi.org/10.1089/jam.1988.1.289.

Oberdörster, G., Oberdörster, E., Oberdörster, J., 2005. Nanotoxicology: an emerging discipline evolving from studies of ultrafine particles. Environ. health Perspect. 113, 823–839. https://doi.org/10.1289/ehp.7339.

Ozdogan, L., Sastim, H., Ornek, D., Ayerden, T., Dikmen, B., 2013. Neurotoxic effects of intrathecal magnesium sulphate. Rev. Bras. Anestesiol. 63 (1), 139–148. https://doi.org/10.1016/S0034-7094(13)70205-8.

Pacella, A., Cremisini, C., Nardi, E., Montereali, M.R., Pettiti, I., Giordani, M., Mattioli, M., Ballirano, P., 2018. Different erionite species bind iron into the structure: a potential explanation for fibrous erionite toxicity. Minerals 8 (2), 36. https://doi.org/10.3390/min8020036.

Parcell, S., 2002. Sulfur in human nutrition and applications in medicine. Alternative Med. Rev. 7 (1), 22–44.

Pedersen, B.K., Bruunsgaard, H., Jensen, M., Toft, A.D., Hansen, H., Ostrowski, K., 1999. Exercise and the immune system-influence of nutrition and ageing. J. Sci. Med. Sport 2 (3), 234–252. https://doi.org/10.1016/S1440-2440(99)80176-5.

Petrault, I., Zimowska, W., Mathieu, J., Bayle, D., Rock, E., Favier, A., Rayssiguier, Y., Mazur, A., 2002. Changes in gene expression in rat thymocytes identified by cDNA array support the occurrence of oxidative stress in early magnesium deficiency. Biochim. Biophys. Acta (BBA) - Mol. Basis Dis. 1586 (1), 92–98. https://doi.org/10.1016/S0925-4439(01)00089-8.

Petriglieri, J.R., Laporte-Magoni, C., Salvioli-Mariani, E., Ferrando, S., Tomatis, M., Fubini, B., Turci, F., 2021. Morphological and chemical properties of fibrous antigorite from lateritic deposit of New Caledonia in view of hazard assessment. Sci. Total Environ. 777 (146185). https://doi.org/10.1016/j.scitotenv.2021.146185.

Pollastri, S., Gualtieri, A.F., Gualtieri, M.L., Hanuskova, M., Cavallo, A., Gaudino, G., 2014. The zeta potential of mineral fibres. J. Hazard Mater. 276, 469–479. https://doi.org/10.1016/j.jhazmat.2014.05.060.

Ribeiro, J., Taffarel, S.R., Sampaio, C.H., Flores, D., Silva, L.F.O., 2013. Mineral speciation and fate of some hazardous contaminants in coal waste pile from anthracite mining in Portugal. Int. J. Coal Geol. 109–110, 15–23. https://doi.org/10.1016/j.coal.2013.01.007.

Roemer, W., Hoek, G., Brunekreef, B., Clench-Aas, J., Forsberg, B., Pekkanen, J., Schutz, A., 2000. PM_{10} elemental composition and acute respiratory health effects in European children (PEACE project). Pollution Effects on Asthmatic Children in Europe. Eur. Respir. J. 15 (3), 553–559.

Roselli, C., Desideri, D., Rongoni, A., Meli, M.A., Feduzi, L., 2015. Radiological Characterization of pharmaceutical and cosmetic clays. J. Radioanal. Nuclear Chem. 303, 2291–2296. https://doi.org/10.1007/s10967-014-3801-y.

Rouse, D.J., Hirtz, D.G., Thom, E., Varner, M.W., Spong, C.Y., Mercer, B.M., Iams, J.D., Wapner, R.J., Sorokin, Y., Alexander, J.M., Harper, M., 2008. A randomized, controlled trial of magnesium sulfate for the prevention of cerebral palsy. N. Engl. J. Med. 359 (9), 895–905. https://doi.org/10.1056/nejmoa0801187.

Roveri, M., Manzi, V., Lucchi, F.R., Rogledi, S., 2003. Sedimentary and tectonic evolution of the Vena del Gesso basin (Northern Apennines, Italy): implications for the onset of the Messinian salinity crisis. Geol. Soc. Am. Bull. 115 (4), 387–405, https://doi.org/10.1130/0016-7606(2003)115<387:SATEOT>2.0.CO;2.

Ruiz-Agudo, E., Putnis, C.V., Rodriguez-Navarro, C., 2008. Interaction between epsomite crystals and organic additives. Cryst. Growth Des. 8 (8), 2665–2673. https://doi.org/10.1021/c.

Salma, I., 2009. Air pollution in underground railway systems. Issues Environ. Sci. Technol. 28, 65–84.

Salma, I., Balásházy, I., Winkler-Heil, R., Hofmann, W., Záray, G., 2002. Effect of particle mass size distribution on the deposition of aerosols in the human respiratory system. J. Aerosol Sci. 33 (1), 119–132. https://doi.org/10.1016/S0021-8502(01)00154-9.

Schuh, S., Sweeney, J., Rumantir, M., Coates, A.L., Willan, A.R., Stephens, D., Atenafu, E.G., Finkelstein, Y., Thompson, G., Zemek, R., Plint, A.C., 2020. Effect of nebulized magnesium vs placebo added to albuterol on hospitalization among children with refractory acute asthma treated in the emergency department: a randomized clinical trial. JAMA 324 (20), 2038–2047. https://doi.org/10.1001/jama.2020.19839.

Schwartz, J., Dockery, D.W., Neas, L.M., 1996. Is daily mortality associated specifically with fine particles? J. Air Waste Manag. Assoc. 46 (10), 927–939. https://doi.org/10.1080/10473289.1996.10467528.

Seiler, R.L., Stillings, L.L., Cutler, N., Salonen, L., Outola, I., 2011. Biogeochemical factors affecting the presence of ^{210}Po in groundwater. Appl. Geochem. 26 (4), 526–539. https://doi.org/10.1016/j.apgeochem.2011.01.011.

Seiler, R.L., Wiemels, J.L., 2012. Occurrence of ^{210}Po and biological effects of low-level exposure: the need for research. Environ. health Perspect. 120 (9), 1230–1237. https://doi.org/10.1289/ehp.1104607.

Srebro, D.P., Vučković, S., Vujović, K.S., Prostran, M., 2014. Anti-hyperalgesic effect of systemic magnesium sulfate in carrageenan-induced inflammatory pain in rats: influence of the nitric oxide pathway. Magnes. Res. 27 (2), 77–85. https://www.jle.com/10.1684/mrh.2014.0364.

Studer, A.M., Limbach, L.K., Van Duc, L., Krumeich, F., Athanassiou, E.K., Gerber, L.C., Moch, H., Stark, W.J., 2010. Nanoparticle cytotoxicity depends on intracellular solubility: comparison of stabilized copper metal and degradable copper oxide nanoparticles. Toxicol. Lett. 197 (3), 169–174. https://doi.org/10.1016/j.toxlet.2010.05.012.

Sturm, R., Hofmann, W., 2009. A theoretical approach to the deposition and clearance of fibers with variable size in the human respiratory tract. J. Hazard Mater. 170 (1), 210–218. https://doi.org/10.1016/j.jhazmat.2009.04.107.

Sturm, R., 2011. Radioactivity and lung cancer-mathematical models of radionuclide deposition in the human lungs. J. Thorac. Dis. 3 (4), 231–243. https://doi.org/10.3978/j.issn.2072-1439.2011.04.01.

Tam, M., Gomez, S., Gonzalez-Gross, M., Marcos, A., 2003. Possible roles of magnesium on the immune system. Eur. J. Clin. Nutr. 57 (10), 1193–1197. https://doi.org/10.1038/sj.ejcn.1601689.

Tam, H.B.T., Dowling, O., Xue, X., Lewis, D., Rochelson, B., Metz, C.N., 2011. Magnesium sulfate ameliorates maternal and fetal inflammation in a rat model of maternal

infection. Am. J. Obstet. Gynecol. 204 (4), 364–e1. https://doi.org/10.1016/j.ajog.2010.11.006.
Thakkar, A.H., 2001. Rapid sequential separation of actinides using Eichrom's extraction chromatographic material. J. Radioanal. Nucl. Chem. 248/2, 453–456. https://doi.org/10.1023/A:1010660915984.
Ueshima, K., Shibata, M., Suzuki, T., Endo, S., Hiramori, K., 2003. Extracellular matrix disturbances in acute myocardial infarction: relation between disease severity and matrix metalloproteinase-1, and effects of magnesium pretreatment on reperfusion injury. Magnes. Res. 16 (2), 120–126.
Vanoeteren, C., Cornelis, R., Sabbioni, E., 1986. Critical Evaluation of Normal Levels of Major and Trace Elements in Human Lung Tissue. Commission of the European Communities, Luxembourg.
Ventura, L.M.B., Mateus, V.L., de Almeida, A.C.S.L., Wanderley, K.B., Taira, F.T., Saint'Pierre, T.D., Gioda, A., 2017. Chemical composition of fine particles (PM 2.5): water-soluble organic fraction and trace metals. Air Quality. Atmos. Health 10 (7), 845–852. https://doi.org/10.1007/s11869-017-0474-z.
Wei, B., Yang, L., Zhu, O., Yu, J., Jia, X., Dong, T., Lu, R., 2014. Multivariate analysis of trace elements distribution in hair of pleural plaques patients and health group in a rural area from China. Hair Ther. Transplant. 4 (2), 1–7.
World Health Organization (WHO), 1999. Occupational and Environmental Health Team;. Hazard Prevention and Control in the Work Environment. Report WHO/SDE/OEH/99.14, Geneva airborne dust.
World Health Organization (WHO), 1986. Asbestos and Other Natural Mineral Fibers; Environmental Health Criteria, ume 53. Switzerland, Geneva, pp. 69–107 1986.
Wise, W.S., Tschernich, R.W., 1976. The chemical compositions and origin of the zeolites offretite, erionite, and levyne. Am. Mineral. 61 (9–10), 853–863.
Wright, J.W., Ridgway, L.E., Wright, B.D., Covington, D.L., Bobitt, J.R., 1996. Effect of $MgSO_4$ on heart rate monitoring in the preterm fetus. J. Reprod. Med. 41 (8), 605–608.
Wu, X., Kassie, F., Mersch-Sundermann, V., 2005. Induction of apoptosis in tumor cells by naturally occurring sulfur-containing compounds. Mutat. Res. Rev. Mutat. Res. 589 (2), 81–102. https://doi.org/10.1016/j.mrrev.2004.11.001.
Xia, Y., Bo, A., Liu, Z., Chi, B., Su, Z., Hu, Y., Luo, R., Su, X., Sun, J., 2016. Effects of magnesium sulfate on apoptosis in cultured human gastric epithelial cells. Food Agric. Immunol. 27 (2), 171–181. https://doi.org/10.1080/09540105.2015.1079596.
Zhang, X., Bo, A., Chi, B., Xia, Y., Su, X., Sun, J., 2015. Magnesium sulfate induced toxicity in vitro in AGS gastric adenocarcinoma cells and in vivo in mouse gastric mucosa. Asian Pac. J. Cancer Prev. APJCP 16 (1), 71–76. https://doi.org/10.7314/APJCP.2015.16.1.71.